Design Considerations for a Strain Actuated Adaptive Wing for Aeroelastic Control

CHARRISSA Y. LIN* AND EDWARD F. CRAWLEY
M.I.T. Space Engineering Research Center, 77 Massachusetts Ave., Rm. 37-341, Cambridge, MA 02139

ABSTRACT: The dominant issues in the preliminary design of a strain actuated aeroelastic wing are examined. First, the scaling parameter for piezoelectric actuation authority is obtained and used to extrapolate strain actuation variables from an earlier model. Second, the interaction of composite fiber angle and geometric sweep angle is studied, specifically the effect of these parameters on the passive aeroelastic behavior and potential closed-loop actuation authority. Finally, a taper ratio trade is completed to understand the effect of varying taper ratio on the passive and active aeroelastic characteristics.

INTRODUCTION

In recent decades, one of the focuses of aeroelastic research has been the control of aeroelastic behavior. The objectives have included delaying the onset of instability, achieving ride control or vibration suppression, and providing maneuver and performance enhancement. The vast majority of active aeroelastic control experiments to date have used conventional flap actuators. However, flaps and ailerons are not necessarily the optimal actuation choice.

As an alternative to conventional flap actuation, strain actuation is being examined for use in aeroelastic control. The primary advantage to strain actuation is that the actuators affect the structure directly by inducing strain in the structure. An additional benefit is that the bandwidth of strain actuators is large compared to the frequencies of structural dynamic deformation. Since strain is induced in the structure directly, there are no associated lags. The use of piezoelectric strain actuators to modify the static aeroelastic behavior has been examined analytically (Ehlers and Weisshaar, 1990) and a two degree of freedom wind tunnel model has been used to demonstrate strain actuated flutter suppression (Heeg, 1992). A plate-like lifting surface with piezoelectric actuators has successfully demonstrated vibration and flutter suppression using multiple input/multiple output controllers (Lazarus and Crawley, 1992).

The principle objective of this project is to demonstrate the utility of strain actuation for aeroelastic control and to compare the effectiveness of strain actuation with conventional control surface actuation. Using both strain and conventional actuators, controllers will be developed to demonstrate suppression of vibration and bending/torsion flutter. This current article summarizes the preliminary design phase of the project, conducted by M.I.T. in cooperation with the NASA Langley Research Center (LaRC), which culminates in the testing of an active wing in the LaRC Transonic Dynamics Tunnel.

To ensure that the stated project objective is met, specific performance requirements must be established. The wing model geometry and properties must be representative of near future aircraft wings in which bending/torsion flutter is critical. In addition, the model is designed such that flutter will occur below static divergence and reversal, and such that the flutter mechanism is a coalescence of the first two modes.

To focus on the aeroelastic control of a more easily modeled plant, the model is designed to flutter well below the transonic speed range, before compressibility becomes a significant factor. To introduce structural thickness and bend-twist coupling without the complications of a monocoque wing structure, the internal structure is a composite sandwich spar construction with a sectioned aerodynamic shell providing realistic aerodynamic contours without adding appreciable stiffness.

The design parameters of the wing model are selected through a series of non-parametric and parametric studies. Not discussed here are the selection of many parameters, which have been determined by comparisons to typical transport aircraft and by manufacturing and wind tunnel constraints (Lin and Crawley, 1993). The more salient design parameters, such as piezoelectric thickness and grouping, composite fiber sweep angle, geometric sweep angle, and the taper ratio, are established by several parametric studies. The first is a scaling analysis which establishes the governing piezoelectric authority scaling parameter and compares the current design with the experimental model used by Lazarus and Crawley (1992). The major parametric study examines the interaction of the fiber sweep angle and the geometric sweep angle and the manner in which they affect the aeroelastic behavior and the actuation effectiveness. As a part of this study, the area coverage of the

Guest Editor: E. Breitbach.

*Author to whom correspondence should be addressed.

1045-389X/95/03 0403-08 $10.00/0

piezoceramic is determined. The final parametric study investigates the effect of varying taper ratios on both the passive aeroelastic behavior and the actuation authority.

SCALING ANALYSIS

Aeroelastic model theory (Bisplinghoff, Ashley and Halfman, 1955) has traditionally identified a number of scaling parameters, which, if properly matched, allow the extrapolation of model results to full scale. With the addition of strain actuation, a new physical element has been added, thus requiring a new scaling parameter. In this section, the new parameter is identified. The parameter is then used to extrapolate the strain actuation authority from Lazarus' test article to the present design, and to determine an appropriate spar thickness ratio and piezoelectric thickness. One of the most important differences between Lazarus' test article and the current investigation is the increase in the structural thickness of the test article and its effect on the piezoelectric authority.

Using energy methods, the governing differential equation for an anisotropic plate-like lifting surface with piezoelectric layers can be derived and appropriately non-dimensionalized (Lin and Crawley, 1993). From these non-dimensional equations a new non-dimensional parameter, which expresses the relative strain actuator authority, is obtained as

$$c_r = \frac{m_{\Lambda_0} L^2}{D_0 w_0} \tag{1}$$

where

m_{Λ_0} = $\int Q_0^a \Lambda_a z dz$ is the piezoelectric actuation moment; Q_0^a is the reference modulus of the actuator layer; Λ_0 is the reference actuation strain
L = span
D_0 = reference stiffness
w_0 = reference displacement

In order to customize the non-dimensional group for a particular application, the length to be used for the reference vertical displacement, w_0, must be chosen. There are three possible choices: the span (L), the semichord (b), and the thickness (h). It is apparent that the nature of the parameter changes with the dimension chosen for w_0. For aeroelastic problems in which the fundamental interest is in controlling the angle of attack of the wing, the choice of b is the natural one, since it equates the non-dimensional parameter with the ability to induce a given twist in the wing. The final scaling parameter and its approximation for a box-beam are

$$c_r = \frac{m_{\Lambda_0} L^2}{D_0 b} = 2\left(\frac{L}{h}\right)\left(\frac{L}{b}\right)\left(\frac{1}{1+\Psi}\right)\Lambda_0 \tag{2}$$

where

$$\Psi = \frac{E_s t_s}{E_a t_a}$$

Note that if a model of a fixed configuration is geometrically scaled and the same materials are used in model and full scale, the parameter is automatically matched.

In the design of a new wing, the methods which can increase the piezoelectric authority are clear. In most problems the substrate modulus, E_s, and the structural aspect ratio, L/b, will be predetermined. Likewise, the modulus, E_a, and actuation strain, Λ_0, of the piezoelectrics is established by the current material technology. Therefore, the thickness of the actuator layer, t_a, and the slenderness ratio, L/h, are the two terms which can be altered to increase the piezoelectric authority.

In the current design, the objective is to meet or exceed the actuation authority of Lazarus' test article (Lazarus and Crawley, 1992). Two authority cases are examined: the first, a bending authority case, which utilizes the bending stiffness for the nominal stiffness, D_0, and the second, a torsional authority case, which utilizes the effective bend-twist stiffness for the nominal stiffness, D_0 (Lazarus and Crawley, 1992).

$$\text{Bending Authority Effective Stiffness } D_0 = D_{11}$$
$$\text{Torsional Authority Effective Stiffness } D_0 = \frac{D_{11}D_{66} - D_{16}^2}{D_{16}} \tag{3}$$

The bending and torsion effective stiffnesses relate the bending and twist displacements to the piezoelectric bending moment, respectively. Because in-plane isotropic piezoelectric actuators can not produce shear strain, the wing design takes advantage of bend-twist coupling to gain authority over torsional motion. Therefore, the torsional authority effective stiffness is not the torsional stiffness, but a bend-twist coupling stiffness.

The most significant difference between Lazarus' test article and the current design is the spar thickness ratio. To incorporate representative structural thickness, the thickness ratio is increased from 0.5% in Lazarus' test article to 2% in the current design. A 2% thickness is chosen as a compromise between realistic spar thickness and the achievable performance of current strain actuation. Because the half-span aspect ratio is also increased from 2 to 4, the slenderness ratio only increases from 0.25% to 0.5%.

The piezoelectric thickness is varied to examine its effect on the relative strain actuation authority parameter. To isolate the effect of the geometrical changes on the relative strain actuation authority parameter, the laminate and material properties of Lazarus' test article are assumed for the current design.

The bending authority comparison (Figure 1) shows that the current design will achieve authority equal to that of

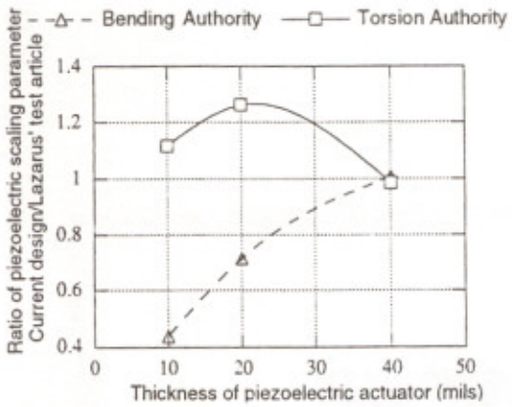

Figure 1. *Comparison of piezoelectric scaling parameters.*

Lazarus' test article for sufficiently thick piezoelectrics. The authority parameter initially increases for increasing piezoelectric thickness by increasing the piezoelectric moment, m_{A_0}. However, increasing the piezoelectric thickness also increases the piezoelectric contribution to the overall stiffness. For further increasing thicknesses, the authority will begin to decrease as the piezoelectric stiffness is proportional to the thickness cubed, while the piezoelectric moment is only proportional to the thickness squared.

The other principle trend observed in Figure 1 is that there exists an optimal thickness for torsional authority. The torsional authority depends upon the bend-twist coupling of the entire structure. Increasing the piezoelectric thickness increases the weighting of the piezoelectric isotropy relative to the anisotropic laminates and the overall isotropy is increased. In the limit, as the structure becomes dominated by piezoelectrics, the structure becomes essentially isotropic and no torsion is induced. Due to these results, a piezoelectric thickness of 0.020 in. and a structural thickness of 2% will be used as baselines for the remainder of the analysis.

FIBER SWEEP AND GEOMETRIC SWEEP TRADE

Geometric sweep and fiber sweep are two of the most influential parametric trades to be made in the aeroelastic design of a wing. Together, they affect the open loop stability and the potential closed loop authority of the strain and flap actuators. The two parameters must be examined simultaneously due to their interactive nature. The motivating requirements in the design are: that the wing model must flutter before it diverges; that the geometric sweep should be representative of transport aircraft with a bending-torsion flutter mechanism; and that independent control of the first two modes is possible using the strain actuators. This section investigates the effects and interaction of these two parameters.

In order to examine these trades, a model is developed using the Rayleigh-Ritz assumed modes method and two-dimensional strip theory aerodynamics. The structural dynamics are referenced to the wing fixed axes $(\bar{x},\bar{y})$ and represent the wing as a rectangular plate even when swept (Figure 2). Five Rayleigh-Ritz assumed shapes are used: two beam bending shapes, two plate torsional shapes, and a chordwise bending shape. The two beam bending shapes are the natural modes of a cantilevered beam (Blevins, 1984). The chordwise bending shape is a free-free beam bending mode in the chordwise direction with a parabolic spanwise distribution. The plate torsional shapes are the torsional modes derived by a partial Ritz method (Crawley and Dugundji, 1980) in the spanwise direction and are linear in the chordwise direction. Using these assumed shape functions, the resulting equations of motion in the structural axes are derived. The homogeneous problem is mass normalized and transformed to modal form.

Following the structural development, the aerodynamics are modeled. Full unsteady, incompressible two dimensional strip theory with a one pole approximation of Theodorsen's function is used. The aerodynamic forces are naturally calculated in the wind axes (x,y) and subsequently transformed to the wing fixed axes $(\bar{x},\bar{y})$ to coincide with the structural dynamics. To avoid the complications of unsteady aerodynamics due to camber, the chordwise mode is not included in the aerodynamics. Appropriate corrections for geometric sweep are made to the aerodynamic forces. The generalized aerodynamic forces are fully transformed into the wing fixed axes, mass normalized, and incorporated into the modal equations of motion. It should be noted that the structural span, not the aerodynamic span, is kept constant when geometrical sweep is varied.

STABILITY TRENDS IN A SIMPLIFIED WING MODEL

Before modeling and analyzing the actual wing design, the aeroelastic stability of simple rectangular plates is examined in order to verify the analytical model and determine dominant parametric trends. The test case of 3″ by 12″ graphite epoxy plates of Landsberger and Dugundji (1985) is used. The lay-up is $[\theta/\theta/0]$s. Figure 3 shows the trends for

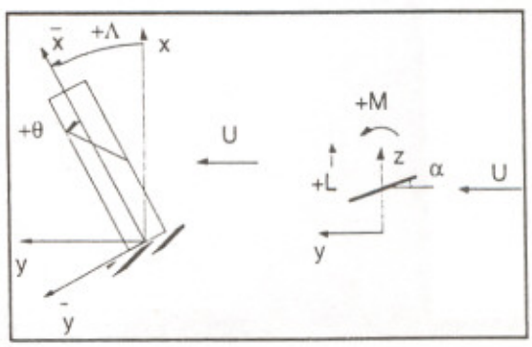

Figure 2. *Sign convention for Rayleigh-Ritz and aerodynamic analysis.*

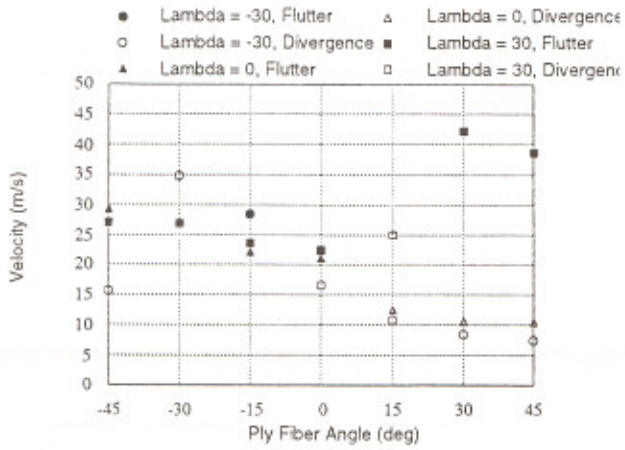

Figure 3. *Calculated flutter and divergence speeds for the ply fiber angle vs. geometric sweep angle trade for the simplified wing model.*

ply fiber angle and structural sweep. This figure matches Landsberger's predicted stability speeds precisely and shows good correlation with the experimental data of Figure 7 in Landsberger and Dugundji (1985).

The flutter and divergence boundaries in Figure 3 are defined by the interaction of the geometric sweep and the fiber sweep. Forward geometric sweep (Λ negative) and aft fiber sweep (θ positive) both create wash-in. Conversely, aft geometric sweep (Λ positive) and forward fiber sweep (θ negative) create wash-out.

Combining forward geometric sweep and aft fiber sweep produces wings which consistently diverge first. The divergence speeds are also robust to small changes in either parameter. In this case, the "wash-in" effect caused by the aft fiber sweep is augmented by a similar effect due to the forward geometric sweep. When the geometric sweep is zero, the aft fiber sweep "wash-in" effect still dominates and these wings also diverge first.

Similarly, aft geometric sweep augments the "wash-out" effects of forward fiber sweep. All of the wings in this portion of the trade space flutter first. In addition, the flutter speeds are robust to small changes in either geometric or fiber sweep. When the geometric sweep is zero, the forward fiber sweep "wash-out" effect dominates and these wings also flutter first.

When the two sweep effects oppose each other, the nature and speed of the first instability encountered are sensitive to small changes in geometric of fiber sweep. The "wash-in" due to forward geometric sweep counteracts the "wash-out" due to forward fiber sweep and the stability boundary for these sweeps is composed of a flutter boundary and a divergence boundary. The same is true when aft geometric sweep is used with aft fiber sweep.

By comparing these trends with the functional requirements, a portion of the trade space is chosen for further examination. The wing is required to flutter before it diverges. The yet-to-be-optimized actuation requirement argues that it is desirable to have a region in which the nature of the first instability and its speed are robust to small changes in geometric and fiber sweep. This reduces the trade space to non-forward geometric sweeps (Λ positive or zero) and non-aft fiber sweeps (θ negative or zero).

STABILITY TRENDS IN THE ACTUAL WING MODEL

Now that the aeroelastic model has been verified and a design subspace identified, a more representative wing model will be analyzed. Figure 4 shows the simplified model of the built-up wing. The structural box has a span of 48 in. and a chord of 12 in. The baseline structural thickness ratio of 2% gives a box thickness of 0.24 in. The same six-ply lay-ups $[\theta_2/0]$s will be used for each facesheet, but the graphite epoxy used will be AS4/3501-6. An aluminum honeycomb serves as the core between the two facesheets and will be modeled as an isotropic material with an elastic modulus two orders of magnitude smaller than the longitudinal modulus of the graphite epoxy.

In addition to the changes in the structural core, there are several new features. A fiberglass aerodynamic shell covering a span of 48 in. and a chord of 15.6 in. is modeled with mass only. Aerodynamically, the wing is considered to be a flat plate. A 20 mil layer of piezoelectrics covers the entire chord but only 60% of the structural box span and is modeled with stiffness and mass. An extra mass section of 0.5 lb. is added to represent the additional mass of flap bearings and supports. An evenly distributed 2.2 lb. tip mass is added to provide for the tip mass flutter stopper. It has the same aerodynamic chord as the wing and adds an extra 3 in. to the span.

The natural modes are calculated using the Rayleigh-Ritz procedure and are listed in Table 1. Because of the mass non uniformity and fiber sweep, all of the modes are linear combinations of the assumed Ritz shapes. In particular, the second and third modes for all of the ply fiber angles except for zero degrees are highly coupled modes containing elements of first torsion and second bending.

Incorporating the aerodynamics, aeroelastic trends similar to those for the simpler rectangular plates appear. Qualitatively, the results replicate the left half of Figure 3 for aft and zero geometric sweep angles (Figure 5). As was found

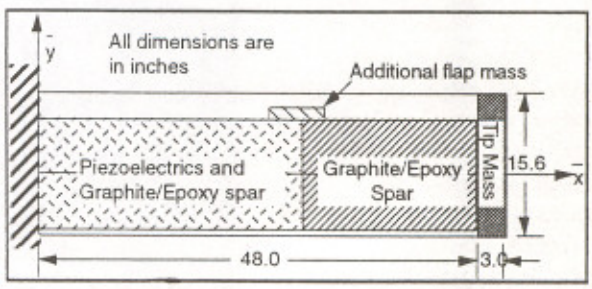

Figure 4. *Schematic of wing model used in analysis.*

Table 1. Natural frequencies for first three modes of wing model (HZ).

Mode	[0/0/90]$_s$	[15/15/0]$_s$	[30/30/0]$_s$	[45/45/0]$_s$
1B	3.3	3.5	3.2	3.0
"2B"	18.8	20.3	16.9	16.5
"1T"	14.4	15.9	19.8	19.2

for the simple rectangular plates, the nature of the first instability and its speed are robust to changes in geometric and fiber sweep for this subspace; therefore, a geometric sweep angle and a fiber sweep angle may be chosen within this subspace to satisfy additional requirements.

The requirement that the flutter mechanism will be a first mode/second mode coalescence will now be enforced. For a given fiber sweep angle, the flutter mechanism does not change appreciably for a change in geometric sweep angle within the design subspace. The flutter mechanisms for fiber sweep angles of 0, −15, and −30 degrees are coalescences of the first two modes. The flutter mechanism for a fiber sweep angle of −45 degrees is a complex three mode mechanism. Therefore, the −45 degree fiber sweep angle will be eliminated from further consideration. The cases of aft geometric sweep and forward fiber sweep of 0 to 30 de- s have shown that they have desirable stability charac- tics and are comparable to transport design practice. The actuation authority requirement is now considered to determine the final angle selections.

ACTUATION TRENDS IN THE ACTUAL WING MODEL

In this section, the effect of the ply fiber angle and structural sweep angle on the actuation authority of the wing model will be studied. One of the primary reasons for choosing a composite laminate is to create bend-twist coupling to enhance the piezoelectric authority on the torsional

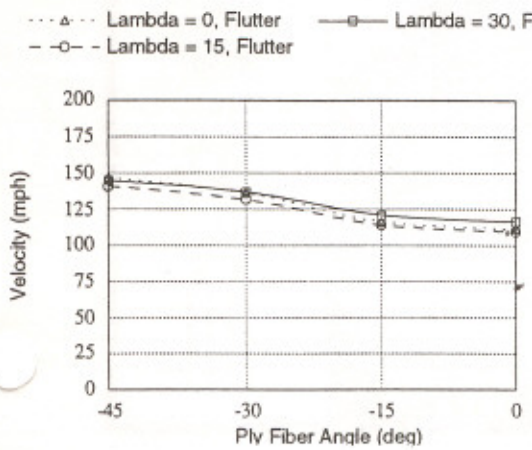

Figure 5. *Flutter speeds for the actual wing model for varying ply fiber angle and geometric sweep angle.*

mode. This must be done without reducing the authority of the trailing edge flap. First, the open loop authority of the actuators is examined and then a closed loop Linear Quadratic Regulator analysis is completed to address the relative performance of the actuators.

To model the generalized forces due to the flap, its sectional aerodynamic forces are calculated. The influence of the flap is included in the aerodynamics which includes one additional lag state. For simplicity, it is assumed that the trailing edge flap is a commanded position surface with perfect oscillatory dynamics. Using this approximation, the flap forces can be expressed solely as a function of the commanded flap angle.

The piezoelectric actuators are modeled as layers of the laminated plate (Crawley and de Luis, 1987). The effect of the piezoelectric induced strain on the mode shapes is determined. High modal controllability is achieved by a piezoelectric when it is placed in an area of high modal strain. To choose basic groupings and locations for the piezoelectric actuators, the bending strain contours of the first two in vacuo natural modes are examined. Attention is focused only on the spanwise bending curvature, since the chordwise bending curvature is roughly two orders of magnitude less than the spanwise curvature and the isotropic piezoelectrics can not exert shear strain. Examining the spanwise bending curvature contours (Figure 6), it is apparent that the inboard portion of the wing is high in strain. Therefore, the piezoelectric actuators are placed from the root to 60% of the span.

For a fiber sweep angle of zero degrees, the only spanwise bending curvature in the second mode is concentrated in the corners of the root and are due to root warping. For fiber sweep angles of −15 and −30 degrees, there are higher levels of spanwise bending curvature in the second mode due to the bend-twist coupling. Figure 6 shows the strain contours for a fiber sweep angle of −15 degrees which is also representative of the strain distribution for a fiber sweep angle of −30 degrees. This implies that the piezoelectrics will be able to exert more effective control over the second mode for these fiber sweep angles than for the zero degree fiber sweep angle. Because of this increased authority over the second mode, attention is focused on the fiber sweep angles of −15 and −30 degrees.

For the present purposes, the piezoelectric coverage is divided into two areas of actuator effectiveness. In typical section studies (Lazarus, Crawley, and Lin, 1991), it has been shown that at least two independent actuators are necessary to provide effective aeroelastic control. For the fiber sweep angles of −15 and −30 degrees, there is a curvature node line in the spanwise bending curvature of the second mode at roughly 30% of the span. This indicates that dividing the piezoelectric coverage in half spanwise would create two "actuators" that can control the first two modes independently: acting together to actuate the first mode and opposing each other to actuate the second. This defines the inboard piezoelectric bank to cover from the root to 30% of

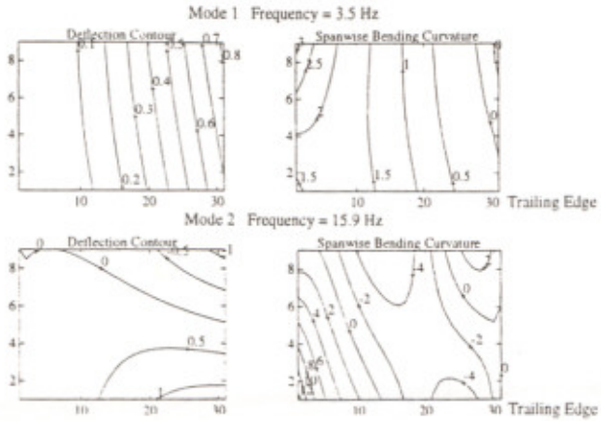

Figure 6. *Deflection and curvature contours for the two primary modes of the actual wing model with a* $[-15/-15/0]_s$ *laminate.*

the span and the outboard piezoelectric bank to cover from 30% to 60% of the span. These fiber sweep angles also avoid placing the node line of the second mode near the trailing edge flap. This insures reasonable flap authority on the first two modes.

The final step of this trade study is to evaluate the relative performance of the piezoelectric and flap actuators by designing a series of full state feedback controllers. Controllers will be designed using the Linear Quadratic Regulator (LQR) method for each of the three actuators (the two piezoelectric actuation areas and the trailing edge flap) alone and all three actuators together. Performance is evaluated at the flutter speed of the model. For all cases, the state penalty is on the displacement states of the first two modes, which are weighted equally. All other states are weighted at zero. The controls are weighted with representative maximum values: 20 V/mil for the piezoelectric actuators and $+/-1$ degree for the trailing edge flap. The 20 V/mil field is approximately the coercive field of the piezoelectric.

Cost curves are used to compare the controllers. The covariance of the weighted states comprises the state cost and the covariance of the weighted control inputs comprises the control cost. To compute the covariance, a disturbance is created by implementing an angle of attack variation. The disturbance intensity is 0.1 degrees.

Using a geometric sweep angle of 30 degrees, the effect of fiber sweep angle on actuator authority can be seen in Figure 7. For each fiber sweep angle, it can be seen that the inboard piezoelectric actuation area has the best performance (i.e., lowest state cost for a given control cost). The trailing edge flap and the outboard piezoelectric actuation area have nearly equivalent performance.

The relative performance of the piezoelectric actuators as compared to the trailing edge flap in Figure 7 qualitatively matches the relative performance of the actuators predicted by a typical section analysis (Lazarus, Crawley, and Lin, 1991). In both cases, one of the piezoelectric actuators outperformed the aerodynamic control surface. A detailed comparison of the two can be found in Lin and Crawley (Lin and Crawley, 1993). A notable discrepancy with the typical section work (Lazarus, Crawley, and Lin, 1991) lies in the performance improvement when using all three actuators. In the typical section, the controller using all three actuators performed significantly better than any of the single actuator controller designs over all control cost regions. In Figure 7 it can be seen that the controller using all three actuators performs only slightly better than the best single actuator controller design in the low control cost region. This can be explained by examining the flutter mechanisms in the two problems. The typical section has a perfect two mode coalescence. Therefore, it is important to exert effective control over both of the modes, independently and in equal magnitude. In the current design, the flutter mechanism is dominated by the first mode. Therefore, most of the gain in performance is achieved by exerting effective control over the first mode.

Although the single actuators perform well in the low control cost region, each of the single actuator curves has a horizontal asymptote in the high control cost region. In contrast, the combination of three actuators has no such limit. This inherent performance limit of a single actuator has been seen in the typical section analyses and demonstrates that effective high authority aeroelastic control requires at least two actuators (Lazarus and Crawley, 1992; Lazarus, Crawley, and Lin, 1991).

The cost curve comparison (Figure 7) reiterates the benefit of the bend-twist coupling introduced by the fiber sweep angles of -15 and -30 degrees. The single actuator curves of the zero degree fiber sweep angle show equivalent performance to the single actuator curves of the -15 and -30 degree fiber sweeps. However, the strain contours demonstrated that effective control of the second mode requires the two piezoelectric actuation areas acting in opposition. This indicates that the single actuator cases are only controlling the first mode effectively. The benefit of bend-twist coupling is most clearly seen in the cost curves of the

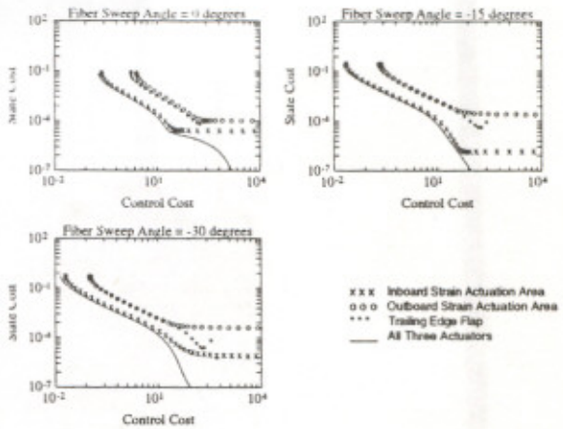

Figure 7. *Cost curves for the wing model at a geometric sweep angle of 30 degrees for varying fiber sweep angles. Evaluated at calculated flutter speed.*

three actuators working together. Due to its lack of authority over the second mode, the zero degree fiber sweep with multiple actuators does not improve the performance in the high authority range as well as the corresponding combination for fiber sweep angles of −15 and −30 degrees. Therefore, the zero degree fiber sweep is eliminated from consideration. From the two remaining angles, a baseline fiber sweep angle of −15 degrees is chosen, because its second mode more closely resembles a torsional mode than the second mode of the −30 degree fiber sweep angle.

A similar cost curve analysis is performed for varying geometric sweep. The results show that there is virtually no variation in performance for varying aft geometric sweep angles between 0 and 30 degrees. Therefore, a baseline geometric sweep angle of 30 degrees is chosen for similarly to transport aircraft.

TAPER RATIO TRADE

The final trade that is examined in this design process is that of taper ratio. Typical transport wings have tip chords which are considerably smaller than the root chords with taper ratios ranging from 0.30 to 0.16. The taper ratios examined in this chapter range from 1 to 0.5. These taper ratios are intended to resemble a taper ratio of a transport wing if the trailing edge angle in the outer wing panel is continued to the root. This excludes the extra wing area at the trailing edge/fuselage junction area created by a greatly reduced trailing edge angle in the inner wing panel.

The only change in the model from the nominal wing is the taper ratio. The baseline layup of [−15/−15/0]s and the baseline geometric sweep angle of 30 degrees are used. The tip mass remains as it was modeled in the reference model, a 2.2 lb (1 kg) distributed weight. The taper ratio is introduced by holding the tip chord of the spar constant and altering the root chord accordingly. The aspect ratio is reduced by a small amount because of the introduction of taper in this manner. The additional spar area has mass and stiffness properties and, as before, the additional skin area has mass properties only. No piezoelectrics are modeled on the additional spar area. The aerodynamic model also accounts for the tapered chord. The semichord of the midpoint of each strip is used in the strip theory calculations.

Before performing the stability analysis, the natural modes are determined. The frequencies of the first three modes are listed in Table 2. It is apparent that the change in frequencies is not large when the taper ratio is changed in this manner. Likewise, the order in which the modes appear is maintained. The larger the taper ratio, the closer the behavior is to the non-tapered model.

Incorporating the aerodynamics and analyzing the stability of the aeroelastic system, it becomes apparent that the incorporation of taper ratio affects the aeroelastic behavior very little. The flutter speeds for the different taper ratios are also listed in Table 2. The overall change in flutter speed is insignificant. Similarly, the pole loci for the tapered wing models closely resemble the non-tapered model.

Table 2. Natural frequencies and flutter data for tapered and nominal wing models. Lay-up is [−15/−15/0]s. Frequencies in HZ, speed in M/S.

	Taper Ratio			
	0.5	0.67	0.75	1.0
1B	4.1	3.8	3.7	3.5
2B	21.1	20.6	20.6	20.3
1T	15.5	15.7	15.7	15.9
Flutter speed	55.1	54.1	54.0	54.1
Flutter freq.	8.3	7.8	7.7	7.5

Part of this robustness to change in taper ratio is due to the manner in which the taper was introduced. By maintaining the tip dimensions, the effect of the change in taper has been limited. Clearly, the tip and its properties are dominant in determining the dynamic and aeroelastic behavior of the wing. In order to obtain a taper ratio with a representative transport wing profile, a taper ratio of 0.67 is chosen as a reference taper ratio.

As a final step in ensuring that the addition of taper has not altered the wing design appreciably, the effect on the actuator authority is observed for the reference taper ratio of 0.67. The strain contours for the tapered wing model closely resemble the strain contours for the non-tapered wing model. Therefore, the groupings determined for the non-tapered wing model still provide the independent control needed. LQR controllers are designed using the same weightings as before and under the same disturbance. The cost curves calculated for the tapered wing model show no significant changes from the non-tapered wing model's cost curves.

CONCLUSIONS

The main purpose of this study has been to understand the important issues in strain actuated aeroelastic control with the goal of designing a wing model for aeroelastic control experiments. This wing model employs both strain actuators and a conventional flap actuator. Through a series of non-parametric and parametric studies, baseline design parameters have been chosen for the wing model.

First, the additional piezoelectric authority scaling parameter has been identified. This parameter indicates that there is an optimal piezoelectric thickness for torsional authority when using bend/twist coupled laminates. Next, the geometric sweep and fiber sweep have been selected based upon passive and active criterion. The passive aeroelastic analysis has provided a region (aft geometric sweep and forward fiber sweep) in which the first instability encountered is always flutter and the flutter speed is robust to small changes in either parameters. The significance of

this conclusion is that the fiber sweep angle and geometric sweep angle can be optimized within this region with respect to the actuation authority. Third, the control analysis demonstrated that incorporating bend/twist coupling into the structure enables independent control of the torsional mode by the piezoelectric actuators. In the closed-loop control analysis, the performance of the piezoelectric actuators is comparable to the flap actuator. In addition, because the flutter mechanism is dominated by a single mode, most of the performance gain is achieved by effective control of the first mode. A final conclusion resulted from the taper ratio study, which demonstrated that when the tip dimensions are held constant, the dynamics will not alter appreciably.

These studies and their results comprise the preliminary design phase of the strain actuation demonstration experiments. While this study, in addition to previous work, establishes a solid foundation for strain actuated aeroelastic control, much work remains to be done. The strain actuated aeroelastic control technology will benefit greatly from material advances and enhanced strain capability. Along with the material advances, the use of current anisotropic strain actuators and the design of new anisotropic strain actuators to enhance torsional authority should be examined. Finally, before this technology can enter practical usage, the current demonstration phase must be brought to fruition and the technology must be further verified in a realistic monocoque wing structure.

REFERENCES

Bisplinghoff, R. L., H. Ashley and R. L. Halfman. 1955. *Aeroelasticity.* Reading, MA: Addison-Wesley Publishing Company.

Blevins, R. D. 1984. *Formulas for Natural Frequency and Mode Shape.* Malabar, FL: Robert E. Krieger Publishing Company.

Crawley, E. F. and J. de Luis. 1987. "Use of Piezoelectric Actuators as Elements of Intelligent Structures", *AIAA Journal,* 25(10):1373–1385.

Crawley, E. F. and J. Dugundji. 1980. "Frequency Determination and Non-Dimensionalization for Composite Cantilever Plates", *Journal of Sound and Vibration,* 72(1):1–10.

Ehlers, S. M. and T. A. Weisshaar. 1990. "Static Aeroelastic Behavior of an Adaptive Laminated Piezoelectric Composite Wing", AIAA Paper No. 90-1078, *Proceedings of the 31st Structure, Structural Dynamics, and Materials Conference,* Long Beach, CA, May, pp. 1611–1623.

Heeg, J. 1992. "An Analytical and Experimental Investigation of Flutter Suppression via Piezoelectric Actuation", AIAA Paper No. 92–2106, *Proceedings of the AIAA Dynamics Specialists Conference,* Dallas, TX, April, pp. 237–247.

Landsberger, B. J. and J. Dugundji. 1985. "Experimental Aeroelastic Behavior of Unswept and Forward-Swept Cantilever Graphite/Epoxy Wings", *Journal of Aircraft,* 22(8):679–686.

Lazarus, K. B. and E. F. Crawley. 1992. "Multivariable High-Authority Control of Plate-Like Active Lifting Surfaces", SERC Report #14-92, Cambridge, MA: Massachusetts Institute of Technology, June.

Lazarus, K. B., E. F. Crawley and C. Y. Lin. 1991. "Fundamental Mechanisms of Aeroelastic Control with Control Surface and Strain Actuation", AIAA Paper No. 91-0985, *Proceedings of the 33rd AIAA/ASME/ASCE/AHS Structures, Structural Dynamics, and Materials Conference,* Baltimore, MD, April, pp. 1817–1831.

Lin, C. Y. and E. F. Crawley. 1993. "Strain Actuated Aeroelastic Control", SERC Report #2-93, Cambridge, MA: Massachusetts Institute of Technology, February.